Supplementary Information

submitted to *Journal of Materials Chemistry A*

Coral-Like Hierarchical Carbon Nanoarchitectures Loaded with Rh- and Co- Porphyrins as High-Efficiency Electrodes: Effect of Pore Morphology on CO Oxidation and Oxygen Reduction Performance

Shiori Kubo,[a*] *Akira Endo,*[a] *Shin-ichi Yamazaki*[b]

a. Research Institute for Chemical Process Technology, National Institute of Advanced Industrial Science and Technology (AIST), 1-1-1, Higashi, Tsukuba, 305-8561, Japan

b. Research Institute of Electrochemical Energy, AIST, 1-8-31, Midorigaoka, Ikeda, Osaka, 563-0026, Japan

Details of materials characterization and electrochemical measurement techniques

Nitrogen sorption analysis:

Nitrogen (N_2) gas sorption analysis was carried out using Belsorp Max and Belsorp Max II systems (MicrotracBEL Corp.) at 77 K. Each sample was held under vacuum at 180 °C for 2 h and then outgassed to < 7 E-5 Pa prior to measurement. Brunauer-Emmett-Teller (BET), *t*-plot, and Barrett-Joyner-Halenda (BJH) calculations were performed using BelMasterTM version 6.1.0.8. BJH distributions were interpolated by B-Spline interpolation.

Method for calculating $V_{meso\text{-}macro}{}^{*}$:

$$V_{meso-macro}{}^{*}\ [cm^3\ g^{-1}] = V_{meso-macro}[cm^3\ g^{-1}] - V_{cavitation}\ [cm^3\ g^{-1}] \quad \textbf{(S1)}$$

$$V_{cavitation} = \frac{V_{des@0.5}\,[cm^3\,g^{-1}] \times 10^{-3}}{C\,[L\,mol^{-1}]} \times \frac{M\,[g\,mol^{-1}]}{D\,[g\,cm^{-3}]}$$

,where

,where $V_{des@0.5}$ is the V_{ads}^{N2}@STP value at the $P/P_0 = 0.5$ point of the desorption curve of the N_2 isotherms *(i.e.*, relative pressure at which the cavitation event occurs)

, and where

C: the ideal gas constant

M: molecular weight of nitrogen molecule,

and

D: density of liquid nitrogen.

Taking $C = 22.4$ [L mol^{-1}], $M = 28$ [g mol^{-1}], and $D = 0.808$ [g cm^{-1}], $V_{cavitation}$ is calculated by:

$$V_{cavitation} = \frac{V_{des@0.5}\,[cm^3\,g^{-1}] \times 10^{-3}}{22.4\,[L\,mol^{-1}]} \times \frac{28\,[g\,mol^{-1}]}{0.808\,[g\,cm^{-3}]}$$

Electrochemical measurements:

The generation of H_2O_2 during oxygen reduction reaction (ORR) was measured using the modified RRDE and a bi-potentiostat (ALS electrochemical analyzer Model 711B). The potential of the ring Pt electrode was fixed at 1.1 V *vs.* Ag|AgCl|KCl(sat.). This potential is high enough for the Pt ring electrode to oxidize H_2O_2 electrochemically. The ratio of the H_2O_2 generation (X_{H2O2}) was calculated based on **equation S2**.

$$X_{H_2O_2} = \frac{2I_R/N}{I_D + I_R/N} \quad \textbf{(S2)}$$

, where I_R, I_D, and N denote the ring current, disk current, and collection efficiency, respectively. The N value is the ratio of the ring current and disk current of a hydrodynamic voltammogram of $[Fe(CN)_6]^{3-}$ at 6400 rpm.

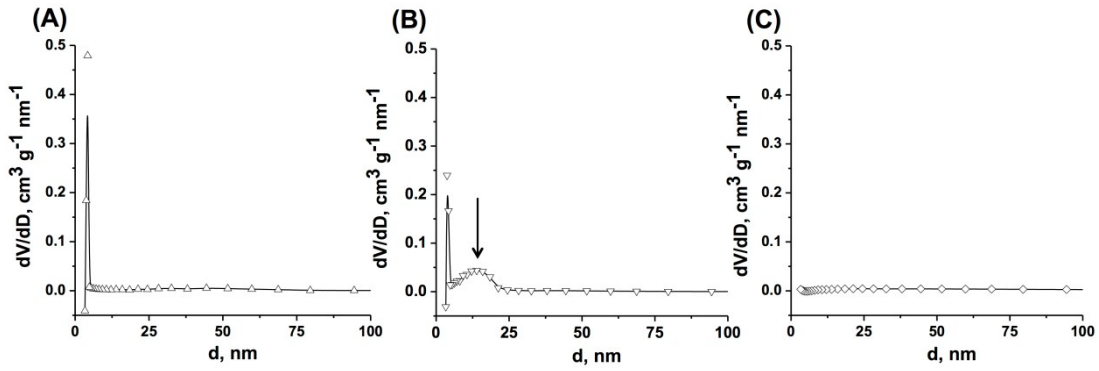

Figure S1. BJH pore size distributions of (A) $C_{micro\text{-}meso}$**_1**, (B) $C_{micro\text{-}meso}$**_2**, and (C) C_{micro}**_3** calculated from the desorption curve.

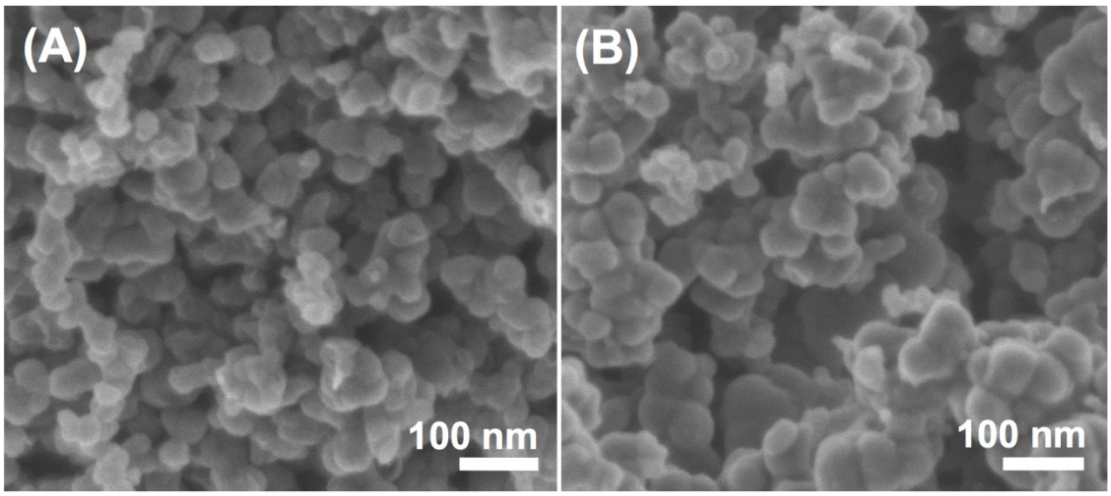

Figure S2. SEM micrographs of (A) Ketjenblack and (B) Vulcan XC 72R commercial carbon samples.

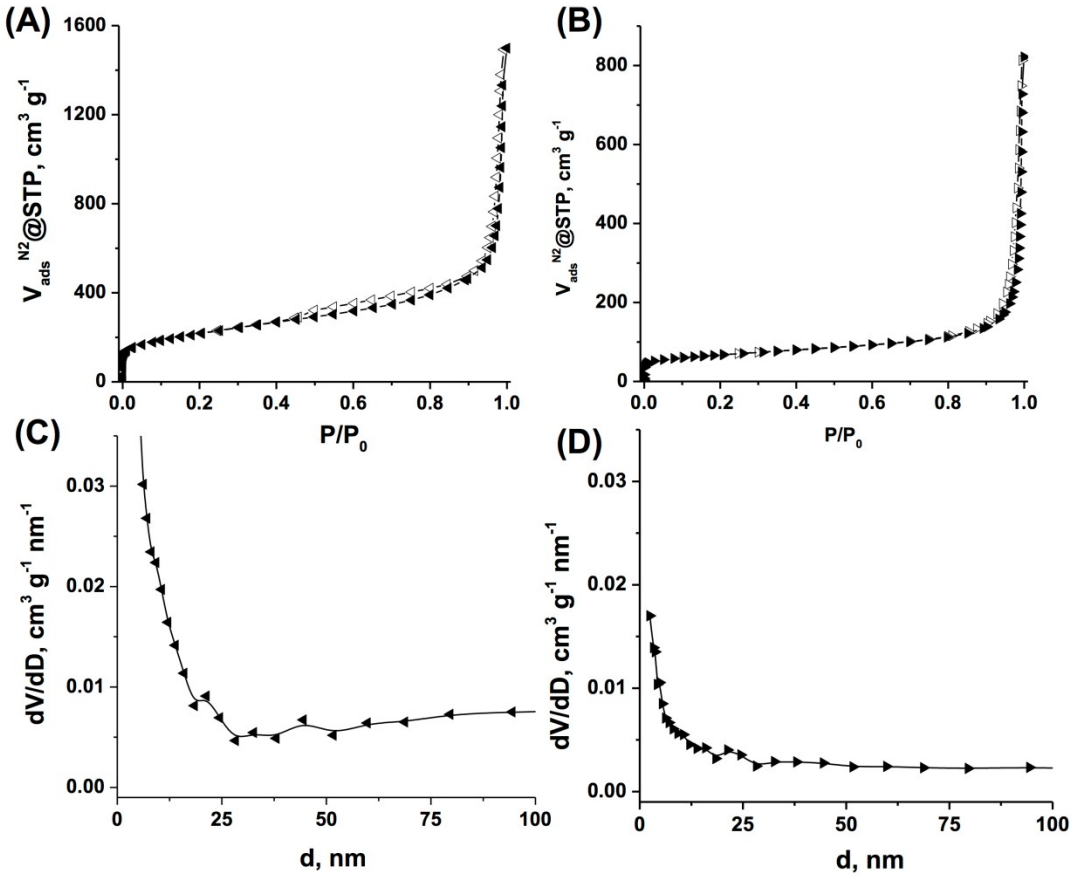

Figure S3. N_2 sorption isotherms (upper stage) and BJH pore size distribution (lower stage) of (A,C) Ketjenblack and (B,D) Vulcan XC 72R.

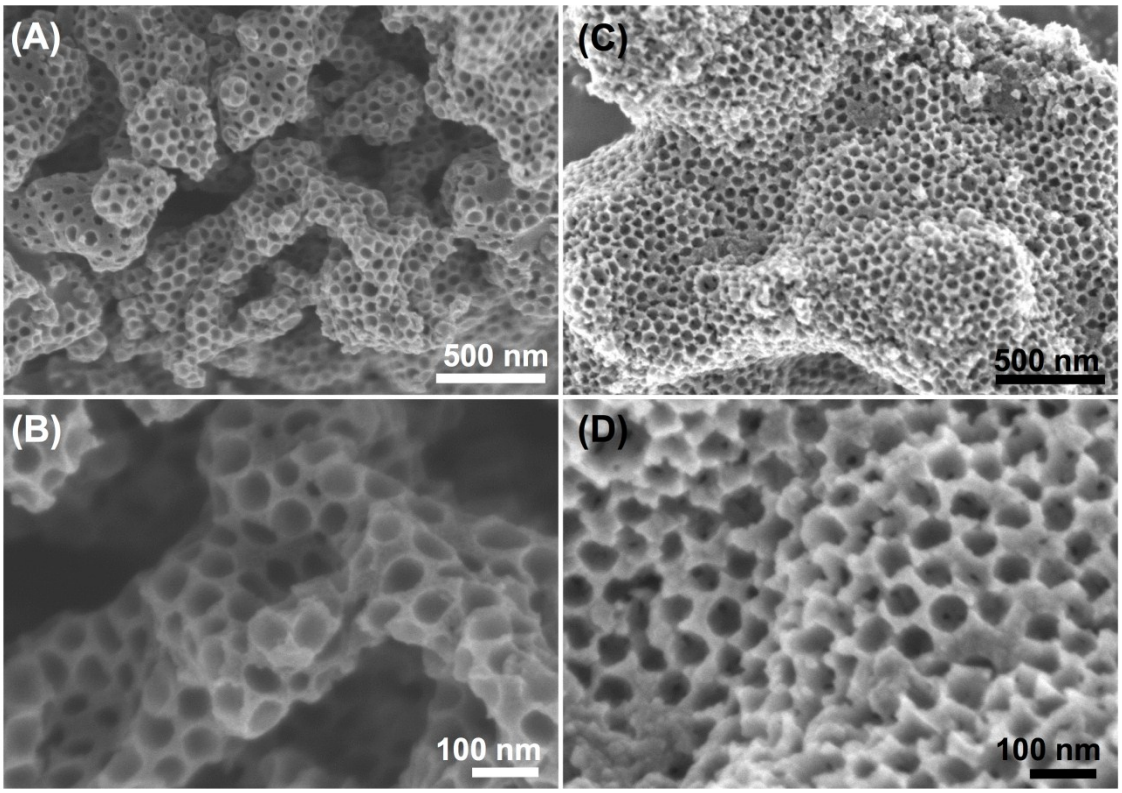

Figure S4. SEM micrograph of coral-like carbon supports pulverized with a spatula (A,B) $C_{micro-meso}$**_1** (C,D) $C_{micro-meso}$**_2**.

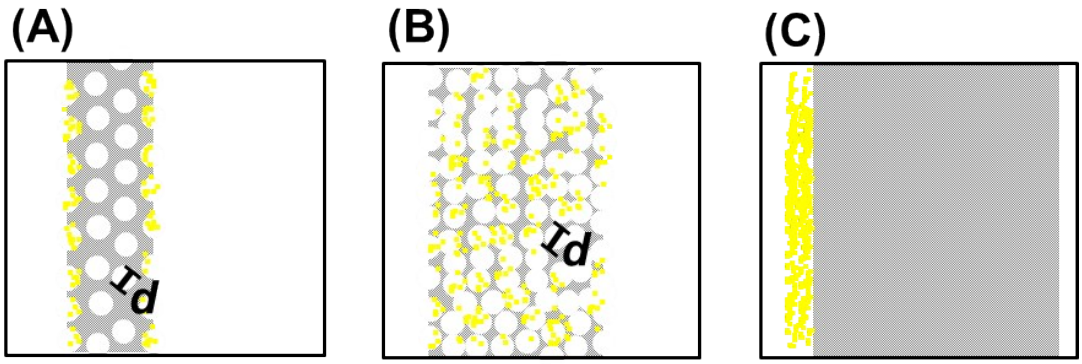

Figure S5. Adsorption model of porphyrin molecules in the spherical pores of (A) $C_{micro-meso}$**_1** and (B) $C_{micro-meso}$**_2** and (C) at particle surface of C_{micro}**_3**. The grey shading indicates the carbon wall (with < 2 nm pores), while the white pores have a diameter (*d*) of ~50 nm. The yellow dots represent porphyrin molecules.

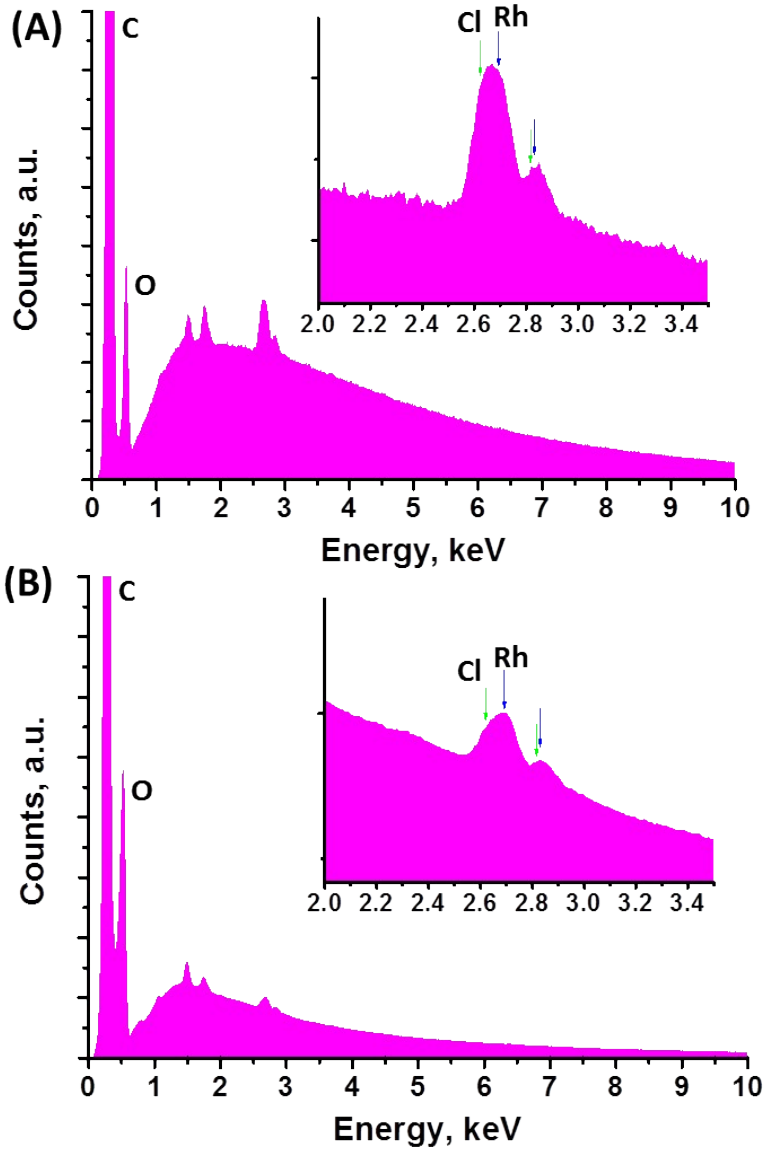

Figure S6. EDX spectra of Rh-TCPP-loaded (A) $C_{micro\text{-}meso}$_**1** and (B) $C_{micro\text{-}meso}$_**2.** Each insert represents the enlarged spectrum of the 2-3.5 keV region, while green and blue arrows represent the positions of the theoretically calculated energy of characteristic X-ray deriving from Cl (Kα, Kβ) and Rh (Lα, Lβ), respectively.

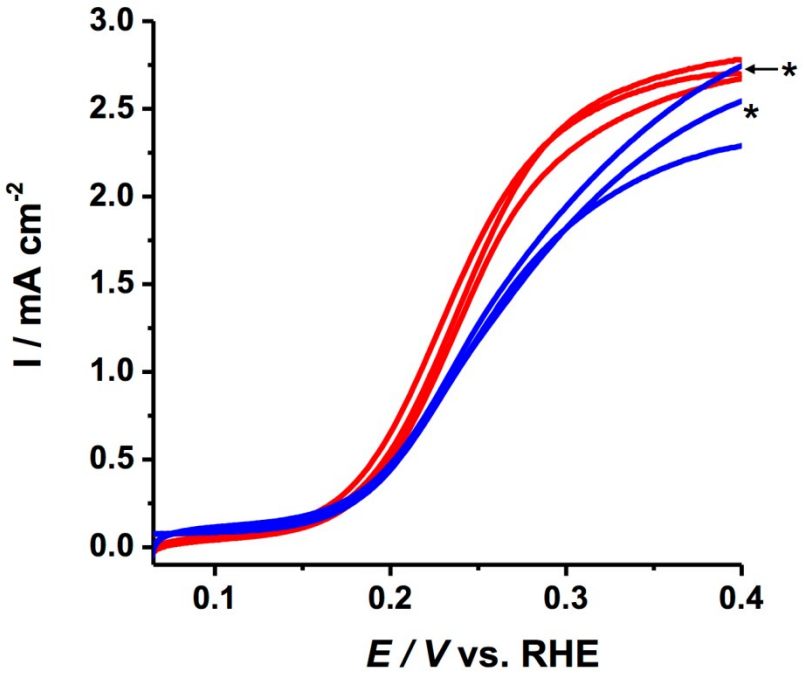

Figure S7. Linear sweep voltammograms of CO oxidation reaction by Rh-TCPP loaded on (blue lines) $C_{micro\text{-}meso}$_**1** and (red lines) $C_{micro\text{-}meso}$_**2** using the evaporation-to-dryness method. Each line corresponds to a voltammogram of the newly prepared modified electrode each time. Starred voltammograms correspond to those shown in Figure 6.

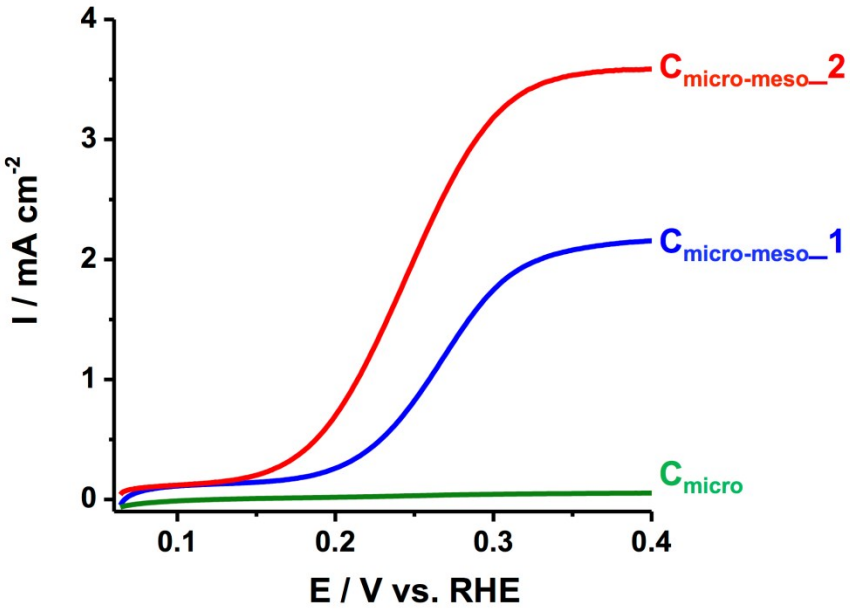

Figure S8. Linear sweep voltammograms for the electrochemical CO oxidation reaction by Rh-TCPP loaded on $C_{micro\text{-}meso}$_**1**, $C_{micro\text{-}meso}$_**2**, and C_{micro}_**3** using the equilibrium adsorption method.

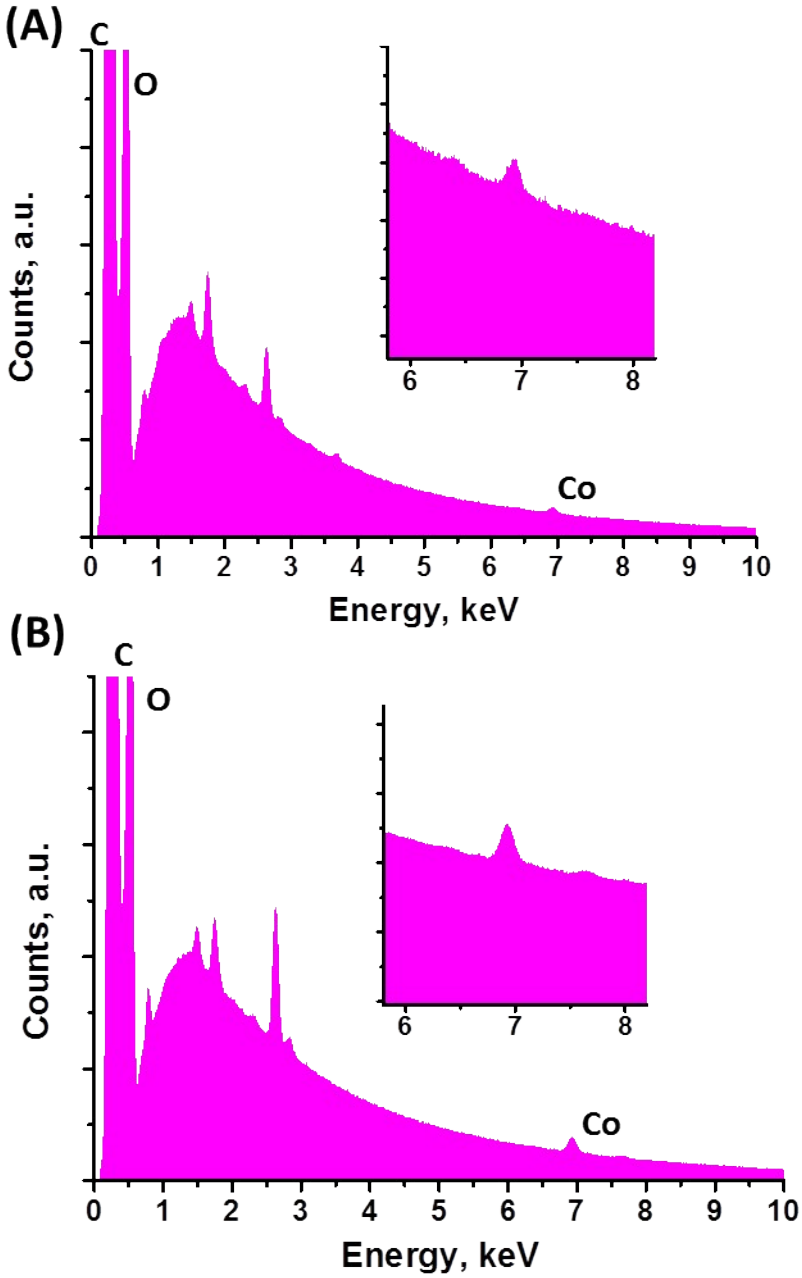

Figure S9. EDX spectra of Co-OEP-loaded (A) $C_{micro\text{-}meso}$_**1** and (B) $C_{micro\text{-}meso}$_**2.** Each insert represents the enlarged spectrum of the 6-8 keV region.

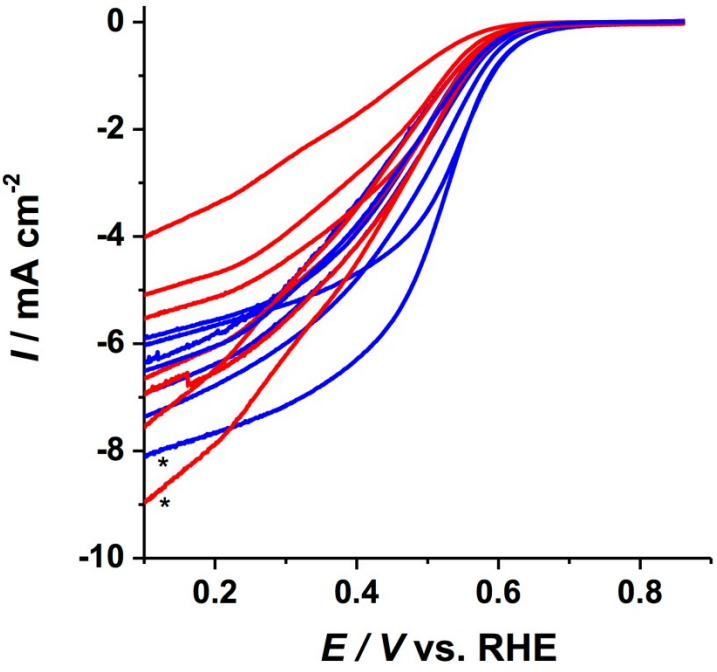

Figure S10. Linear sweep voltammograms of O_2 reduction reaction by Co-OEP loaded on (blue lines) $C_{micro\text{-}meso}$**_1** and (red lines) $C_{micro\text{-}meso}$**_2** using the evaporation-to-dryness method. Each line corresponds to a voltammogram of the newly prepared modified electrode each time. Starred voltammograms correspond to those shown in Figure 7.

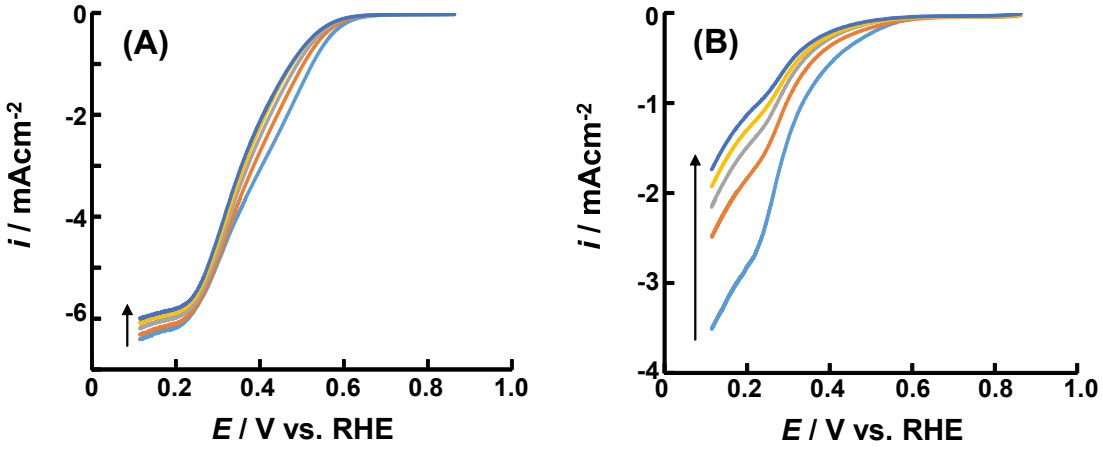

Figure S11. Repeated scans of linear sweep voltammograms of the electrochemical O_2 reduction reaction by Co-OEP loaded on (A) $C_{micro\text{-}meso}$**_1** and (B) Ketjenblack.

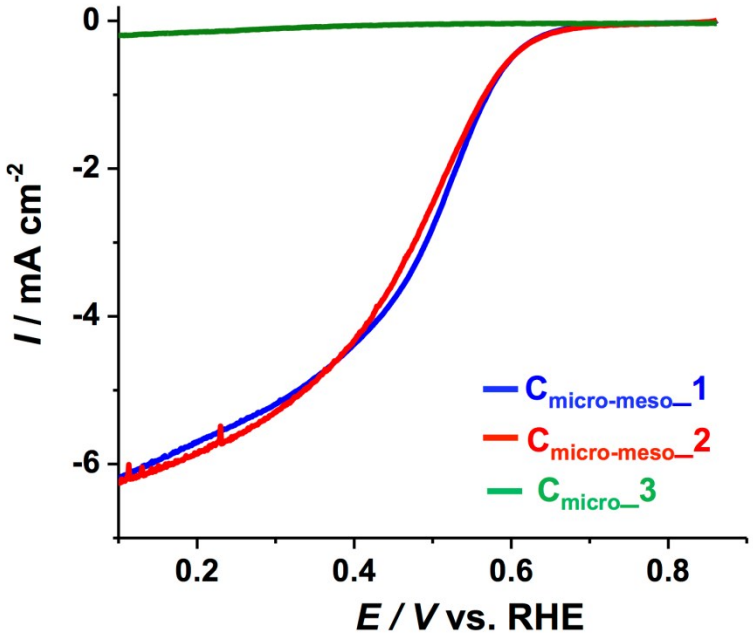

Figure S12. Linear sweep voltammograms of the electrochemical O_2 reduction reaction by Co-OEP loaded on $C_{micro\text{-}meso}$**_1**, $C_{micro\text{-}meso}$**_2** and C_{micro}**_3** using the equilibrium adsorption method.